

Feasibility of Design One-Part Sodium Silicate Activated Metamontmorillonite-Limestone Cements

Nailia R. Rakhimova^{1,*}, Vladimir P. Morozov², Aleksey A. Eskin², Bulat M. Galiullin³

* nailia683@gmail.com

¹ Department of Building Materials, Kazan State University of Architecture and Engineering, 1 Zelenaya str., Kazan 420043, Russian Federation

² Department of Mineralogy and Lithology, Kazan Federal University, 18 Kremlyovskaya str., Kazan 420008, Russian Federation

³ Department of Regional Geology and Natural Resources, Kazan Federal University, 18 Kremlyovskaya str., Kazan 420008, Russian Federation

Received: May 2023

Revised: September 2023

Accepted: September 2023

DOI: 10.22068/ijmse.3272

Abstract: This study evaluated the potential of calcined montmorillonite as a primary precursor for one-part alkali-activated cement incorporated with a high percentage of limestone. Comparative studies on the properties of the sodium silicate-activated metakaolin-limestone and meta montmorillonite-limestone fresh and hardened cement pastes depending on several formulation and processing parameters (precursor nature, dosages of limestone and alkali reactant, curing conditions) showed that meta montmorillonite exhibits reactivity comparable to that of metakaolin in the studied cement systems. The mechanical performance of optimal alkali-activated cement formulations consisting of 20- 30% of meta montmorillonite and 70- 80% of limestone is provided by both the reactivity of meta montmorillonite under sodium silicate activation and the filler, nucleation, and chemical effects of the raw limestone. The reaction products and microstructures of alkali-activated meta montmorillonite-limestone cement-based hardened pastes were investigated using thermal, XRD, and SEM/EDS analyses.

Keywords: Metakaolin, Meta montmorillonite, Alkali, Cement

1. INTRODUCTION

Expanding the available raw materials base is one of the key factors of a promising future for sustainable Portland clinker-reduced and non-clinker cement including alkali-activated cement (AACs). Due to achievements in the chemistry of inorganic materials, the range of potentially suitable precursors has changed and expanded continuously throughout the history of AACs. As a result of ongoing studies conducted in this field, clays and calcium (magnesium) carbonate rocks have gained growing attention. Both clays and carbonate rocks in raw and calcined conditions have been widely studied as precursors of AACs, however, the behavior of these materials under alkali activation continues to evolve [1-6]. The interest in these mineral sources is based not only on the large reserves and their ubiquitous availability, but also on their decreased global warming potential, lowered energy consumption, and multifunctional effect on the engineering performance of blended cements and concretes. For a long time, the limestone (LS) was assigned the role of only an inactive filler for AACs. Many studies stated LS's beneficial effect on the

properties of fresh and hardened alkali-activated (AA) blast furnace slag, fly ash, and calcined clay cement. The positive influence effect of calcium/magnesium carbonates on the performance of AACs is based on the filler, nucleation, dilution, and chemical effects, which are conditioned by the chemical-mineralogical compositions of the primary precursors (Ca-free or Ca-rich), the nature and dosage of the alkaline component, and the content and fineness of LS or dolomite [7-14]. However, recent studies have revealed that the chemical reactivity of LS in AA binder systems is undervalued. Ortega-Zavala et al. [15], Aizat et al. [16], Yin et al. [17], Cousture et al. [18], and Lin et al. [19] reported that calcium/magnesium carbonates could be used as a main precursor for AACs. However, LS and dolomite powders display noticeable reactivity only during long-term ageing under a high alkaline dosage or pressure. The low chemical activity made LS reasonable to be used as a secondary precursor in AAC based on the low content of reactive calcined clays. Perez-Cortez et al. designed an AAC based on metakaolin (MK) and LS [20, 21]. The content of LS was as high as 80% in optimal formulation, molar ratios

$\text{Na}_2\text{O}/\text{Al}_2\text{O}_3$ and $\text{SiO}_2/\text{Al}_2\text{O}_3$ were 0.94 and 3.54 (4.7% Na_2O respective to the mass of MK + LS). The compressive strength (CS) of the designed cement after 24 h of treatment at 60°C was 51.9 ± 0.7 MPa. The microstructure of the hardened pastes was a dense matrix of reaction products with partly reacted LS particles, and the main reaction products were mixed calcium-sodium aluminosilicate hydrogel (C, N)-A-S-H with sodium aluminosilicate hydrogel N-A-S-H, aluminium-substituted sodium aluminosilicate hydrogel C-A-S-H, and calcium silicate hydrogel C-S-H. The introduction of LS to sodium silicate-activated MK decreased alkali component consumption and changed the chemistry and assemblage of the reaction products. The main reaction products were the mixed gels of N-A-S-H and (N-(C)-A-S-H) with 3D network structures where Ca^{2+} replaced Na^+ via an ion-exchange mechanism. Authors stated that compared to Portland cement, the optimal formulation emits 75.1% less CO_2 , consumes 41.1% less energy and is 42.6% less expensive; while compared to the AAC of 100% MK, the reductions were 51.6, 53.8 and 57.5%, respectively. Meanwhile, the properties of the proposed fresh and hardened AAC pastes were not comprehensively investigated, only the CS of the hardened samples was the focus.

The high cost and scarcity of the high-grade MK clay deposits have intensified worldwide the research on evaluating the potential of relatively more abundant clay minerals including montmorillonite [17-20]. Meanwhile, the literature lacks data on the feasibility results of bentonite clay-limestone blends for the purpose of one-part AACs production.

This research work focused on studying:

- The possibility of using calcined bentonite clay as a primary precursor for one-part AAC with a high content of LS,
- Studying the effects of influencing factors, namely percentage of LS, dosage of alkali reactant, and curing conditions on the performance of fresh and hardened pastes, and

reaction products of one-part AACs obtained from calcined montmorillonite and LS.

2. EXPERIMENTAL PROCEDURES

The commercial MK ($d_{50} = 15.2 \mu\text{m}$), metamontmorillonite (MM, thermally activated bentonite clay at 800°C for 1 h, $d_{50} = 14.8 \mu\text{m}$), and LS ($d_{50} = 9.5 \mu\text{m}$), were applied in this study to prepare the AAC paste samples. The chemical compositions of the starting materials are listed in Table 1. The mineral components (%) of raw and calcined bentonite clay are montmorillonite (39), quartz (15), albite (12), mica (11), clinocllore (8), hornblende (7), microcline (6), and calcite (2) (Fig. 1). Anhydrous solid sodium metasilicate (SSM) Na_2SiO_3 was used as the alkali activator in dry form.

The dry mixes of MM or MK with LS and SSM were kneaded for approximately 10 min with water. The fresh pastes were manually cast into $25 \times 25 \times 25$ mm cubic moulds and vibrated for 1 min to remove entrapped air. The workability of the fresh pastes was evaluated using flow-table tests according to EN 1015-3. The water/binder ratio was regulated to maintain constant flowability ranging from 29.5 to 30.0 cm. The fresh pastes were placed into a standard conical ring, and free flow without jolting was allowed. Two perpendicular diameters were determined, and the mean value was recorded as the slump flow. The initial and final setting times were measured using the Vicat needle method according to EN 196-3. The determined values are the averages of three samples. Two sets of samples were then prepared for mechanical tests. The compressive strength (CS) of hardened AAC pastes was tested after steam curing, following a thermal curing program of 24 h of presetting, 4 h to reach the desired temperature, 12 h of dwell time at 80°C , and 3 h of cooling. Mechanical tests were conducted by applying a vertical load between the two parallel surfaces during casting. Each CS determination quoted was based on the average of six measurements from the same cast.

Table 1. Chemical composition of starting materials

Starting material	Component (mass % as oxide)								
	SiO_2	Al_2O_3	Fe_2O_3	CaO	Na_2O	K_2O	MgO	other oxides	LOI
Bentonite clay	53.97	20.13	5.84	1.88	0.35	-	2.44	6.25	9.14
Metakaolin	53.2	43.0	2.2	-	-	-	-	-	1.6
Limestone	14.26	2.44	1.11	43.31	0.38	0.51	0.84	5.77	31.38



Fig. 1. X-ray diffraction patterns of raw and calcined bentonite clay

X-ray diffraction (XRD) and thermal analyses (TG/DSC) were conducted on ground clays and AAC-hardened pastes. The XRD results were obtained using a D2 Phaser X-ray diffractometer in a Bragg-Brentano θ - 2θ configuration with Cu K α radiation operating at 40 kV and 30 mA. Data analysis was performed using the DIFFRAC plus Evaluation Package EVA Search/Match and PDF-2 ICDD database. The mineralogical composition of the clays was determined by analyzing the X-ray diffractograms of the software product Diffrac.eva V3.2. An STA 443 F3 Jupiter simultaneous thermal analysis apparatus was used for the TG/DSC. The clays and hardened AAC pastes were heated from 30°C to 1000°C at a heating rate of 10°C/min. The data were analyzed using Netzsch Proteus Thermal Analysis software. Scanning electron microscopy (SEM; FEI XL-30ESEM) was performed at an accelerating voltage of 20 keV.

3. RESULTS AND DISCUSSION

3.1. Properties of Fresh and Hardened AAC Pastes Based on MK or MM and LSP

Fig. 2(a) presents the CS results of the samples

based on the one-part MM-LS and MK-LS. According to the obtained results, the CS of samples based on both MK and MM is highest when the LS content is in the range of 70–80%, which agrees with the results of Perez-Cortez et al. [20, 21]. An increase of the SSM percentage from 5 to 10% logically positively affects the CS by ensuring higher completeness of the reaction process between precursor and alkali components. However, the CS values of optimal formulations were lower than those obtained by Perez-Cortez et al. [20, 21]. This can be explained by the differences in curing conditions. Curing of the samples at ambient temperature was very slow and resulted in 28 d CS of hardened pastes up to 7.7-10.2 MPa which is consistent with results summarized by Liew et al. [22]. The weak mechanical performance of the samples cured at ambient temperatures is also attributed not only to the slow formation of geopolymer structure but also poor chemical activity of LS. Steam curing significantly intensifies the transformation process of precursors-alkali reactant into binder gel. As a result, steam-cured AAC samples are superior in CS to cured at ambient temperature hardened pastes.



Fig. 2. The influence of the quantity of LS, curing conditions, and SSM dosage on the properties of the MM- and MK-LS hardened (a), fresh MM-LS (SSM - 10% by Na₂O) (b) AAC pastes

The improvement in CS followed by an increase in LS replacement up to 70-80% is probably attributed to several reasons: (i) the filler effect of LS provides better packing density of precursors particles; (ii) an increase in the SSM/reactive phase ratio at higher LS dosages against the backdrop of poor chemical activity of LS intensifies the transformation process pace of reactive phase of calcined clays and alkali reactant into binder gel. It is supposed the SSM/reactive phase ratio reaches optimal value for the formation of the continuous mineral matrix with CS and in a volume sufficient to solidify the high content of LS. The CS values of MK-based samples are slightly higher compared to those for MM-based ones which is attributed to the structural differences causing lower reactivity of MM compared to MK. The drastic changes in the CS of the hardened pastes with a percentage LS of more than 80% are probably also explained by the interruption of the continuity of the geopolymer mineral matrix accompanied by a slow reactivity of LS.

The replacement of MM by LS due to its dilution effect decreased the water/binder ratio from 0.7 to 0.55. The setting of the fresh paste shortened setting times - initial from 44 to 16 min, and the final from 69 to 32 min (Fig. 2b).

3.2. Reaction Products and Microstructure of Hardened Pastes

The results of the X-ray diffraction, thermal, and SEM/EDS analyses are shown in Figs. 3 and 4, performed for the optimal formulations of AAC hardened pastes based on MM and MK incorporated with 80% limestone and activated by SSM (10% by Na₂O).

According to XRD results, the main reaction product of hardened pastes both derived from MK and MM, based on the amorphous hump which is centralized between 26 and 29°2 θ , is a gel-like product, indicating the formation of aluminosilicate binder gel, along with relic unreacted quartz, mica, and calcite.

The binder hydrate gel formation is also supported by results obtained through thermal and SEM/EDS analyses. The water loss of 4.52% detected in the area of 50–175°C reflects water evaporation and dehydration from the gel reaction product. The same character of X-ray diffractograms for MM and MK-based samples suggests the formation of N-A-S-H and N-(C)-A-S-H mixed gels as it was stated for sodium silicate-activated MK-LS cement systems. This is also supported by results obtained through thermal and SEM/EDS analyses. The almost equal total mass loss values

as well as those in the area of 50–175°C for MM- and MK-LS samples, which reflect water evaporation and dehydration from the gel reaction product, can be considered as an indicator of the

nearly equal amounts of binder gels formed in both systems. However, the reactive phase composition in MM-LS system requires further more detailed investigation.

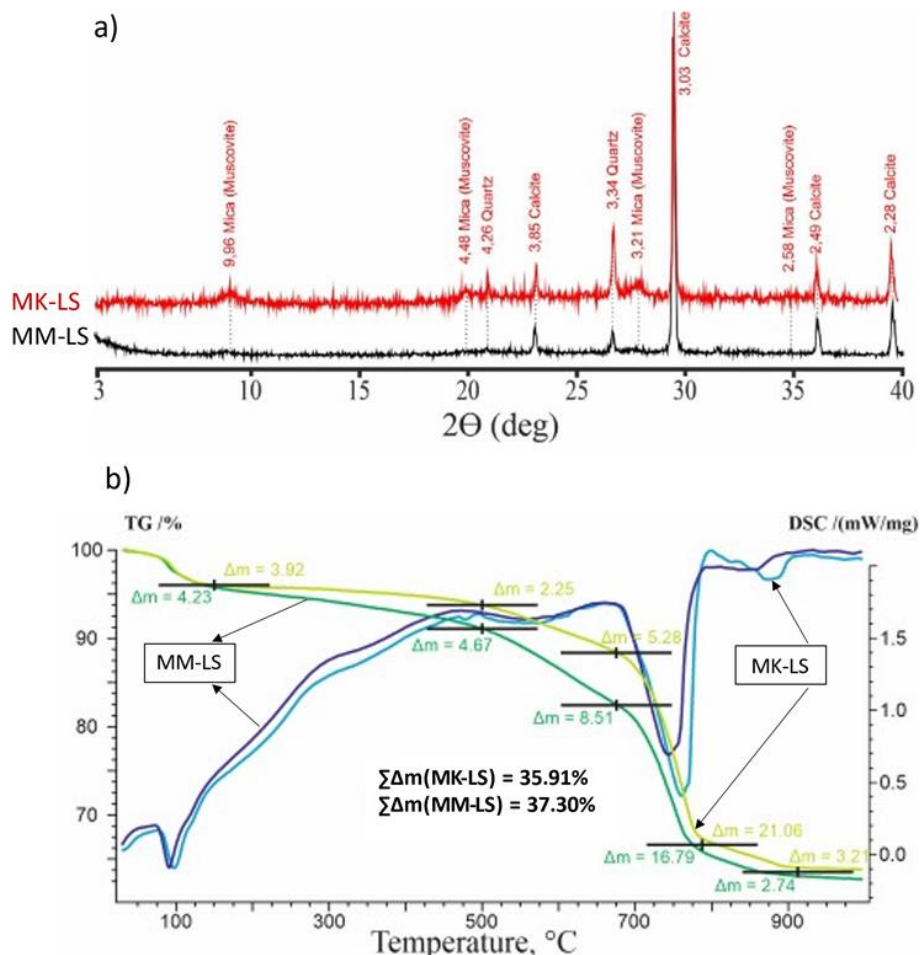


Fig. 3. X-ray diffractograms (a) and thermal analyses (TG/DSC) (b) of hardened pastes

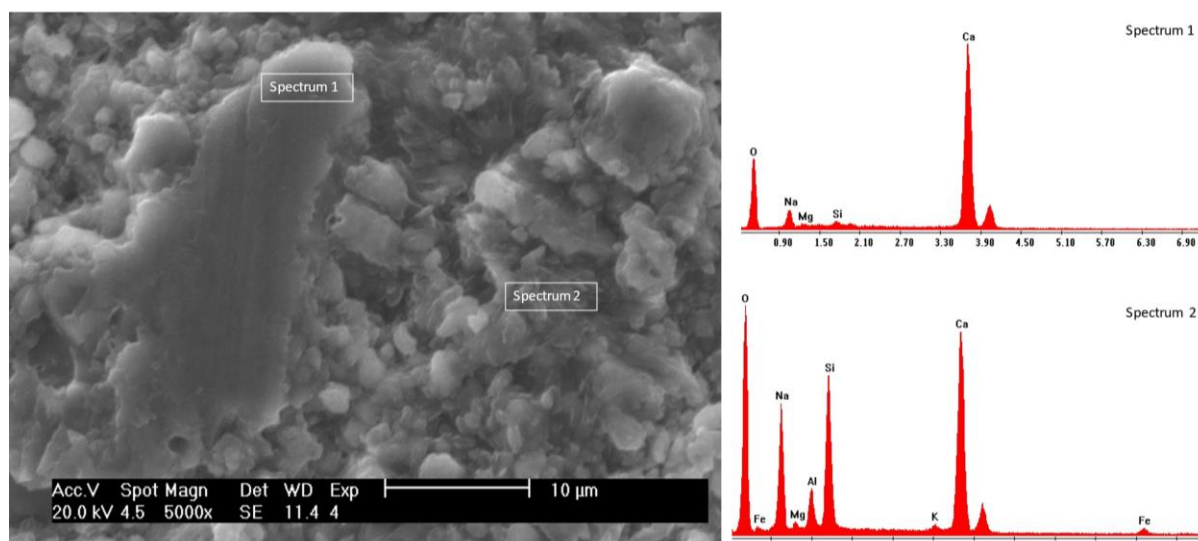


Fig. 4. SEM/EDS images of MM-LS hardened pastes

4. CONCLUSIONS

The results of comparative studies on MM and MK as a primary precursors in one-part AACs incorporated with high percentage of LS are presented in this study. Thermally activated at 800°C bentonite clay at content of clay minerals 39% can be used in combination with LS for one-part AAC production. The incorporation of LS into AACs based on MM decreased water demand, shortened setting times, and improved mechanical performance. Optimal formulations consisted of 20- 30% of MM and 70- 80% LS had a CS up to 32 MPa. The effect of LS on the properties of fresh AAC pastes was based on the dilution effect. The strengthening effect of LS was based on filler, nucleation, and chemical effects. The increase of alkali reactant content from 5 to 10% by Na₂O, and curing at elevated temperatures improved the mechanical performance of proposed SSM-activated MM-limestone cements.

In the designed AAC based on the binary precursor calcined clay-LS, calcined clay is the main reactive precursor that forms a mineral matrix in the form of sodium aluminosilicate hydrate gel N-A-S-H, whereas calcium carbonate is a much less reactive secondary precursor that modifies the main binder gel by forming sodium (calcium) aluminosilicate hydrate gel N-(C)-A-S-H. An intermixed mineral matrix consisting of N-A-S-H and N-(C)-A-S-H gels binds the LS particles by forming a consolidated material. The effect of LS on the properties of fresh AAC pastes which manifests in water demand and setting times of blended fresh AAC paste reduce was based on the dilution effect. The strengthening effect of LS was based on filler, nucleation, and chemical effects.

High content of raw LS contributes to low energy consumption of the proposed AACs. Presented results contribute to the further expanding of the raw materials base for sustainable cements.

REFERENCES

- [1]. Rakhimova, N., "Calcium and/or magnesium carbonate and carbonate-bearing rocks in the development of alkali-activated cements – A review." *Constr. Build. Mater.*, 2022, 325, 26742.
- [2]. Khalifa, A. Z., Cizer, Ö., Pontikes, Y., Heath, A., Patureau, P., Bernal, S. A., Marsh, Al. T. M., "Advances in alkali-activation of clay minerals." *Cem. Concr. Res.*, 2020, 132, 106050.
- [3]. Marsh, A., Heath, A., Patureau, P., Evernden, M., Walker, P., "Alkali activation behaviour of un-calcined montmorillonite and illite clay minerals." *Appl. Clay Sci.*, 2018, 166, 250–261.
- [4]. Garg, N., Skibsted, J., "Dissolution kinetics of calcined kaolinite and montmorillonite in alkaline conditions: Evidence for reactive Al (V) sites." *J. Amer. Ceram. Soc.*, 2019, 102(12), 7720–7734.
- [5]. Rakhimova, N. R., Rakhimov, R. Z., Bikmukhametov, A. R., Morozov, V. P., Eskin, A. A., Lygina, T. Z., Gubaidullina, A. M., "Role of Clay Minerals Content and Calcite in Alkali Activation of Low-Grade Multimineral Clays." *J. Mater. Civil Eng.*, 2020, 32(8), 04020198.
- [6]. Garcia- Lodeiro, I., Boudissa, N., Fernandez-Jimenez, A., Palomo, A., "Use of clays in alkaline hybrid cement preparation. The role of bentonites." *Mater. Lett.*, 2018, 233, 134-137.
- [7]. Zhu, X., Kang, X., Deng, J., Yang, K., Jiang, S., Yang, C., "Chemical and physical effects of high-volume limestone powder on sodium silicate-activated slag cement (AASC)." *Constr. Build. Mater.*, 2021, 292, 123257.
- [8]. Rakhimova, N. R., Rakhimov, R. Z., Naumkina, N. I., Khuzin, A. F., Osin, Y. N., "Influence of limestone content, fineness, and composition on the properties and microstructure of alkali-activated slag cement." *Cem. Concr. Compos.*, 2016, 72, 268–274.
- [9]. Cohen, E., Peled, A., Bar-Nes, G., "Dolomite-based quarry-dust as a substitute for fly-ash geopolymers and cement pastes." *J. Clean. Prod.*, 2019, 235, 910–919.
- [10]. Kalinkin, A. M., Gurevich, B. I., Kalinkina, E. V., Chislov, M. V., Zvereva, I. A., "Geopolymers based on mechanically activated fly ash blended with dolomite." *Miner.*, 2021, 11(7), 700.
- [11]. Alghamdi, H., Nair, S. A. O., Neithalath, N., "Insights into material design, extrusion rheology, and properties of 3D-

- printable alkali-activated fly ash-based binders.” *Mater. Design.*, 2019, 167, 107634.
- [12]. Yamb, E., Kaze, R.C., Nzengwa, R., “Effect of limestone dosages on some properties of geopolymer from thermally activated halloysite.” *Constr. Build. Mater.*, 2019, 217, 28–35.
- [13]. Aboulayt, A., Riahi, M., Ouazzani Touhami, M., Hannache, H., Gomina, M., Moussa, R., “Properties of metakaolin based geopolymer incorporating calcium carbonate.” *Adv. Powd. Techn.*, 2017, 28(9), 2393–2401.
- [14]. Qian, J., Song, M. Study on influence of limestone powder on the fresh and hardened properties of early age metakaolin based geopolymer. Springer. Dordrecht. 2015.
- [15]. Ortega-Zavala, D., Santana-Carrillo, J. L., Burciaga-Díaz, O., Escalante-García, J. I., “An initial study on alkali activated limestone binders.” *Cem. Concr. Res.*, 2019, 120, 267–278.
- [16]. Aizat, E. A., Al Bakri, A. M. M., Liew, Y. M., Heah, C. Y., “Chemical composition and strength of dolomite geopolymer composites”: AIP Conference Proceedings 3rd Electronic and Green Materials International Conference, 020192-1–020192-4, 2017.
- [17]. Yin, Q., Wen, Z.Y. Reaction between carbonaceous rocks and water glass. 12th International Congress on the Chemistry of Cement. Montreal Canada. 2007. p. 5.
- [18]. Cousture, A., Gallias, J.-L., “Study of a binder based on alkaline activated limestone.” *Constr. Build. Mater.*, 2021, 311, 125323.
- [19]. Lin, W., Zhou, F., Luo, W., You, L., “Recycling the waste dolomite powder with excellent consolidation properties: Sample synthesis, mechanical evaluation, and consolidation mechanism analysis.” *Constr. Build. Mater.*, 2021, 290, 123198.
- [20]. Perez-Cortes, P., Ivan Escalante-Garcia, J., “Design and optimization of alkaline binders of limestone-metakaolin – A comparison of strength, microstructure and sustainability with portland cement and geopolymers.” *J. Clean. Prod.*, 2020, 273, 123118.
- [21]. Perez-Cortes, P., Escalante-Garcia, J. I., “Alkali activated metakaolin with high limestone contents - statistical modeling of strength and environmental and cost analyses.” *Cem. Concr. Comp.*, 2020, 106, 103450.
- [22]. Liew, Y.-M., Heah, C.-Y., Mohd Mustafa, A. B., & Kamarudin, H. “Structure and properties of clay-based geopolymer cements: A review.” *Progr. Mater. Sci.*, 2016, 83, 595–629.